15

Fluorescence Polarization/Anisotropy Approaches to Study Protein–Ligand Interactions

Effects of Errors and Uncertainties

David M. Jameson and Gabor Mocz

Summary

Fluorescence techniques are widely used in the study of protein–ligand interactions because of their inherent sensitivity, and the fact that they can be implemented at true equilibrium conditions. Fluorescence polarization/anisotropy methodologies, in particular, are now extensively utilized in biotechnology and clinical chemistry. In this chapter, we shall discuss both theoretical and practical aspects of polarization/anisotropy methods. We shall also focus attention on considerations of errors and uncertainties in such measurements, and how these uncertainties affect the ultimate estimation of ligand–protein dissociation constants.

Key Words: Fluorescence; anisotropy; polarization; ligand binding; dissociation constants; error propagation.

1. Introduction

The interactions of proteins with other molecules are responsible for the majority of the molecular complexes which make life possible. Hence, these types of interactions have been the subject of a great many theoretical and experimental studies. The biotechnology and pharmaceutical industries, in particular, have a significant interest in quantifying the number and strengths of ligand–protein interactions. Such quantification requires knowledge of the number of interacting molecular species (stoichiometry) and the strengths of the binding interactions (free energies). The Gibbs free energy associated with a particular binding interaction is related to the dissociation constant by **Eq. 1**:

$$\Delta G = -RT \ln K_d \qquad (1)$$

From: *Methods in Molecular Biology, vol. 305: Protein–Ligand Interactions: Methods and Applications*
Edited by: G. U. Nienhaus © Humana Press Inc., Totowa, NJ

where R is the universal gas constant, T is the temperature, and K_d is the dissociation constant (which is the reciprocal of the association constant). The dissociation constant that characterizes a reversible equilibrium between a protein and a ligand ($PL \leftrightarrow P + L$) is given by:

$$K_d = \frac{[P][L]}{[PL]} \tag{2}$$

To determine K_d, one must thus be able to determine the concentrations of free protein, free ligand, and protein–ligand complex. Because the total protein (P_T) and total ligand (L_T) concentrations are known, the problem reduces to determination of the concentration of the protein–ligand complex (*1,2*). For the case of one binding site, the concentration of protein–ligand complex (PL) is related to K_d, P_T, and L_T via the quadratic equation:

$$[PL] = \frac{(K_d + L_T + P_T) - \sqrt{\left[(K_d + L_T + P_T)^2 - 4P_T L_T\right]}}{2} \tag{3}$$

To determine $[PL]$ in the presence of uncomplexed protein and ligand, optical spectroscopy methods are very popular because they avoid the use of radioactive materials (and hence the attendant health and waste management concerns), and they are generally inexpensive, rapid, and simple. Fluorescence methodologies in particular are extremely sensitive, allowing measurements in the nanomolar to picomolar levels, and given the current commercial availability of literally thousands of fluorescence probes can be applied to almost any protein–ligand system (*see* **ref. 3**). Fluorescence methods may also allow quantification of the complex in the presence of free ligand, i.e., without the need for a separation step such as filtration or chromatography. Such homogeneous methods allow one to study the system at a true equilibrium over a wide range of concentrations. Ideally, in the protein–ligand system being studied, only one component undergoes alterations in its fluorescence signal upon ligand binding. If more than one fluorescence parameter is affected by the binding process, than one unique signal must be isolated by the judicious choice of the excitation and emission wavelengths (for a discussion of optical components such as monochromators and filters *see* **ref. 3**). In many cases, protein–ligand interactions can be studied by following changes in fluorescence intensities of a probe or in the intrinsic fluorescence of the protein subsequent to ligand binding. However, one sometimes encounters systems in which intensity changes do not occur or are minimal (*see* **ref. 4**). The absence of intensity changes upon binding is more common when fluorescence probes with absorption maxima at visible wavelengths are used, which is often necessary to reduce background fluorescence. In such cases, polarization or anisotropy determinations are

extremely useful since they rely upon changes in rotational mobility between free and bound probes. We shall focus our attention exclusively on these techniques.

2. Overview of Polarization/Anisotropy

2.1. Theory

The principles underlying polarization/anisotropy measurements have been described numerous times (*see* **refs.** *3,5–9*), and we shall present only a very brief overview here. Basically, light can be considered as oscillations of an electromagnetic field perpendicular to the direction of propagation - we shall be concerned only with the electric component. Polarizers are optically active devices that can isolate one direction of the electric vector. The most common polarizers used today are 1) dichroic devices, which operate by effectively absorbing one plane of polarization (e.g., Polaroid type-H sheets based on stretched polyvinyl alcohol impregnated with iodine), and 2) double refracting calcite ($CaCO_3$) crystal polarizers—which differentially disperse the two planes of polarization (examples of this class of polarizers are Nicol polarizers, Wollaston prisms, and Glan-type polarizers such as the Glan-Foucault, Glan-Thompson, and Glan-Taylor polarizers). We initially consider that the fluorescence emitted by a sample excited by polarized light can have any direction of polarization. The actual direction of the electric vector of the emission can be determined by viewing the emission through a polarizer, which can be oriented alternatively in the parallel or perpendicular direction relative to the Z axis or laboratory vertical direction. Polarization is then defined as a function of the observed parallel ($I_{\parallel}$) and perpendicular intensities ($I_{\perp}$):

$$P = \frac{I_{\parallel} - I_{\perp}}{I_{\parallel} + I_{\perp}} \tag{4}$$

When plane polarized light of the appropriate wavelength (i.e., a wavelength absorbed by the fluorophore) impinges on a solution of randomly oriented fluorophores a photoselection process occurs. Specifically, the probability (α) of a fluorophore absorbing the incident light (and thus being excited to an upper electronic level) is proportional to the cosine squared of the angle (θ) between the polarization direction of the exciting light and the absorption transition dipole.

$$\alpha = \cos^2\theta \tag{5}$$

If the exciting light is plane polarized parallel to the vertical laboratory axis, then the number of dipoles oriented at an angle, θ, with this vertical axis will be proportional to $\sin\theta$. These two considerations account for the *photoselection* process that occurs when polarized light excites a population of

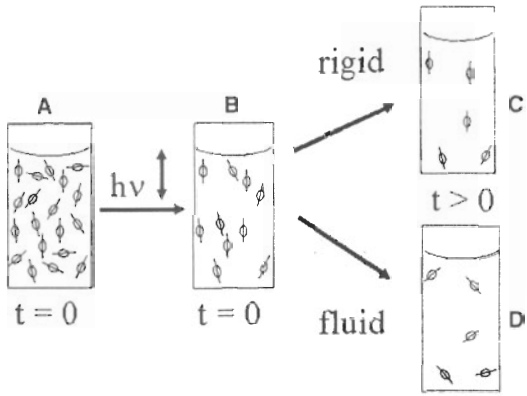

Fig. 1. Depiction of photoselection and rotation of fluorophores. (**A**) depicts a population of fluorophores with their transition dipoles randomly oriented in solution. In (**B**) vertically polarized light impinges on the population and only fluorophores with transition dipoles oriented approximately parallel to the electric vector of the excitation are excited. In (**C**) the solution is considered to be a highly viscous or rigid environment, and after some time has passed the number of excited fluorophores has decreased as a result of the emission process but the orientation of the excited dipoles is unchanged. In (**D**) the solution is considered to be fluid and the dipoles, which remain after the emission process have rotated relative to their initial photoselected orientation.

fluorophores. They also determine the maximum polarization that can be observed from a randomly oriented population of fluorophores that are not free to rotate, e.g., which are immobilized in a very viscous environment. This limiting polarization (in the case where the emission dipole is colinear with the excitation dipole) is + 1/2 (*7*; but *see* **Note 1**).If the fluorophore is excited, it will emit light (fluorescence) after a short duration (known as the fluorescence lifetime) typically on the order of nanoseconds. In aqueous solution at normal temperatures the fluorophore will usually be able to rotate during this time and the direction of the electric vector corresponding to the emitted light will thus be different than that of the exciting light. The direction of this electric vector —usually monitored at right angles to the excitation direction— can then be analyzed. The photoselection and rotation processes are roughly depicted in **Fig. 1**.

Another term frequently used in the context of polarized emission is anisotropy (usually designated as either A or r) which is defined as:

$$r = \frac{I_{\parallel} - I_{\perp}}{I_{\parallel} + 2I_{\perp}} \tag{6}$$

Given the definition of polarization and anisotropy, one can show that:

$$r = \frac{2}{3}\left(\frac{1}{P} - \frac{1}{3}\right)^{-1} \tag{7}$$

or

$$r = \frac{2P}{3 - P} \tag{8}$$

Clearly, the information content in the polarization function and the anisotropy function is essentially identical, and the use of one term or the other is dictated by practical considerations. We also note that the limiting anisotropy, in the case of colinear emission and excitation dipoles, will be + 2/5.

In 1920, F. Weigert was the first to discover that the fluorescence from solutions of dyes was polarized. Specifically, he looked at solutions of fluorescein, eosin, rhodamine, and other dyes and noted the effect of temperature and viscosity on the observed polarization *(10)*. In Weigert's words "Der Polarisationsgrad des Fluorezenzlichtes nimmt mit wachsender Molekulargröße, mit zunehmender Viskosität des Mediums und mit abnehmender Temperatur, also mit Verringerung der Beweglichkeit der Einzelteilchen zu" ("*The degree of the polarization increases with increasing molecular size, with increasing viscosity of the medium and with decreasing temperature, that is with the reduction of the mobility of the single particles*"). Weigert recognized that all of these considerations meant that fluorescence polarization increased as the mobility of the emitting species decreased.

In 1925–1926, Francis Perrin (son of the famous French physicist, Jean Perrin) published several important papers describing a quantitative theory of fluorescence polarization, including what is now considered his classic paper containing most of the essential information that we use to this day *(11)*. Specifically, Perrin related the observed polarization to the excited state lifetime and the rotational diffusion of a fluorophore:

$$\frac{1}{P} - \frac{1}{3} = \left(\frac{1}{P_0} - \frac{1}{3}\right)\left(1 + \frac{RT}{\eta V}\tau\right) \tag{9}$$

In this equation, P is the observed polarization, P_0 is the limiting polarization (the polarization observed in the absence of rotation), R is the universal gas constant, T is the absolute temperature, V is the molar volume of the rotating unit, η is the solvent viscosity, and τ is the excited state lifetime. This expression is often further simplified to:

$$\frac{1}{P} - \frac{1}{3} = \left(\frac{1}{P_0} - \frac{1}{3}\right)\left(1 + \frac{3\tau}{\rho}\right) \tag{10}$$

where ρ is the Debye rotational relaxation time which for a sphere is given as:

$$\rho_0 = \frac{3\eta V}{RT} \tag{11}$$

In the case of a protein wherein the partial specific volume (v) and hydration (h) are known one can then write:

$$\rho_0 = \frac{3\eta M(v+h)}{RT} \tag{12}$$

where M is the molecular weight, v the partial specific volume, and h the degree of hydration (*see* **Note 2**). The relationship between observed polarization and the rotational mobility of the fluorophore is what makes fluorescence polarization so useful for studies of protein–ligand interactions. The basic idea is simply that the polarization/anisotropy of a fluorescent ligand, free in solution, is low (assuming that the fluorescent lifetime is not extremely short; *see* **Note 2**) but upon binding to a macromolecule, such as a protein, the observed polarization/anisotropy of the fluorescent ligand will increase as a result of its slower rotational mobility. This fact was realized by Laurence who was the first to apply the method to study the interaction of ligands with proteins *(12)*. Specifically, Laurence studied the binding of numerous dyes, including fluorescein, eosin, acridine, and others, to bovine serum albumin and used the polarization data to estimate the binding constants. Dandliker and his coworkers later applied these principles explicitly to study antibody–antigen *(13)* and hormone-binding site interactions *(14)*. One of the first commercial instrument designed for clinical chemistry applications of fluorescence polarization was the TDx instrument from Abbott Laboratories *(15)*.

2.2. Additivity of Polarization/Anisotropy

In order to convert the observed polarization/anisotropy from a mixture of free and bound fluorophore into the fraction of bound ligand we must understand the additivity properties of the relevant functions. The Perrin relationship was extended by Gregorio Weber to consider ellipsoids of revolution with fluorophores attached in random orientations *(16)*. In this study, Weber also explicitly derived the relationship governing additivity of polarizations from different species, namely:

$$\left(\frac{1}{\langle P\rangle} - \frac{1}{3}\right)^{-1} = \sum f_i \left(\frac{1}{P_i} - \frac{1}{3}\right)^{-1} \tag{13}$$

where P is the actual polarization observed arising from i components, f_i represents the fractional contribution of the i^{th} component to the total emission intensity, and P_i is the polarization of the i^{th} component (*see* **Note 3**). This additivity principle was later expressed in terms of anisotropy (r) by Jablonski *(17)* as:

$$r_0 = \sum f_i r_i \tag{14}$$

Although the anisotropy formulation is simpler in appearance, the information content of the two approaches is identical, and given present day computer-assisted data analysis the difference is moot. Clearly, if the quantum yield of the fluorophore changes upon binding, the fractional intensity terms in Weber's additivity equation (**Eq. 13**) will alter. Although many probes (such as fluorescein) do not significantly alter their quantum yield upon interaction with proteins, one should not take this fact for granted and would be well advised to check. If the quantum yield does in fact change, one can readily correct the fitting equation to take the yield change into account. In terms of anisotropy the correct expression relating observed anisotropy (r) to fraction of bound ligand (x), bound anisotropy (r_b), free anisotropy (r_f), and the quantum yield enhancement factor (g) is *(18)*:

$$x = \frac{r - r_f}{r_b - r_f + (g-1)(r_b - r)} \tag{15}$$

An analogous expression can be derived for polarization measurements:

$$x = \frac{(3 - P_b)(P - P_f)}{(3 - P)(P_b - P_f) + (g-1)(3 - P_f)(P_b - P)} \tag{16}$$

where P_f is the polarization of the ligand free in solution, P_b is the polarization of the bound ligand and P is the observed polarization. We note that although this equation is slightly more complex than the corresponding anisotropy equation, given the fact that such data is universally analyzed using computer programs this apparent complexity is moot.

2.3. Practical Considerations

Clearly, every researcher will have his or her unique system to investigate and it would be impossible to give a particular *recipe* for applying polarization/anisotropy methodologies, which would be appropriate for all cases. Nonetheless, certain general considerations apply to all such studies and can be enumerated.The most critical consideration is probably the choice of fluorophore. In applications to ligand–proteins interactions, one will ideally have a fluorescent ligand (although one could conceivably use the intrinsic fluorescence of the protein if that is appreciably altered by the binding of a nonfluorescent ligand) *(19)*. Because most ligand systems are nonfluorescent one must find a way to introduce fluorescence into the system. This problem is usually solved by reacting a fluorophore, which has an appropriately reactive chemical group, with the ligand. It is now possible to find fluorophores with the appropriate reactivity for almost any ligand functional group (*see* **Note 5**). Jameson and Eccleston, to give but one example, have reviewed the methodologies for

attaching fluorescent probes to the sugar moieties of nucleotides *(20)*. Another critical consideration (alluded to earlier) is the fluorescent lifetime of the fluorophore. As evident from Perrin's equation (**Eq. 9**), the observed polarization will depend not only on the rotational rates of the system but also on the excited state lifetimes. Put simply, if the lifetime is too short (relative to the rotational relaxation times involved) the change in polarization or anisotropy may be negligible (*see* **Note 2**). Ideally, one should choose a lifetime such that the polarization/anisotropy of the free ligand is low (typically a lifetime of several nanoseconds will be sufficient) whereas the polarization/anisotropy of the bound ligand is as large as possible, i.e., near the limiting values (P_0 or r_0). Generally, the lifetimes of the most common probes, e.g., in the fluorescein or rhodamine families, will achieve these goals. However, some popular cyanine and Alexa probes may have very short lifetimes. The reader is urged to either find appropriate lifetime values in the primary literature or to contact the company providing the probe for lifetime information. Aspects of time-resolved fluorescence that impact on studies of ligand–protein interactions, were discussed by Jameson and Sawyer *(20)*. Once the fluorescent ligand is in hand, it then remains to simply measure the polarization/anisotropy function at varying ligand–protein ratios. To obtain the complete ligand dissociation curve, an appropriate method is to start with a solution of the fluorescent ligand in the presence of an excess of protein. One then removes part of the ligand–protein solution and replaces it with an equivalent volume of the ligand solution at the same concentration. Hence, the ligand concentration is kept constant while the protein concentration is decreased. In this manner, one can obtain a complete binding curve as shown in the simulations in **Fig. 2**. **Figure 2A** shows typical curves for polarization or anisotropy data as a function of total protein concentration, whereas **Fig. 2B** demonstrates the effect of quantum yield changes (i.e., enhancement values) on the observed data.

3. Sources of Errors

3.1. Overview

The most fundamental source of error in studies of ligand–protein interactions using fluorescence polarization/anisotropy determinations would be actual errors in the polarization measurements themselves. In the days before the commercial availability of fluorescence polarization instruments one had to be particularly aware of such considerations. Researchers now usually trust the manufacturer to provide an accurate instrument. However, knowledge of the potential sources of errors in the apparatus is still useful, and can certainly guide the design of the next generation of instruments.In his classic report of the first photoelectric polarization instrument *(21)*, Gregorio Weber presented a careful and detailed consideration of potential sources of errors in the polar-

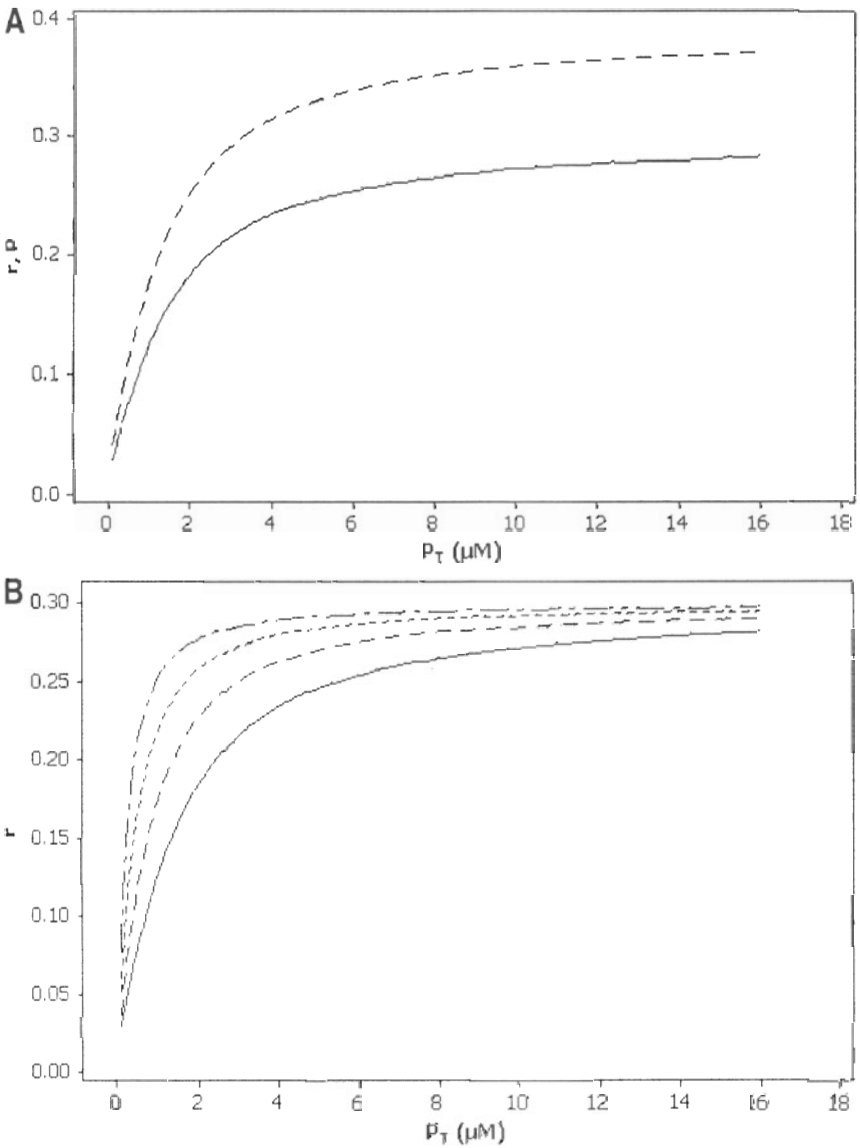

Fig. 2. Simulated titrations of a fluorescent ligand with a protein: anisotropy (r) and polarization (P) vs total protein concentration (P_T). The parameters used in all simulations were: $K_d = 1\ \mu M$, $L_T = 1\ \mu M$, $P_T = 0.0625\ \mu M$ to $16\ \mu M$. $r_f = 0.02$, $r_b = 0.3$. (**A**) solid line: anisotropy, $g = 1$; long dashes: polarization, $g = 1$; (**B**) solid line: anisotropy, $g = 1$; long dashes: anisotropy, $g = 2$; dashes: anisotropy, $g = 4$; dash-dot: anisotropy, $g = 8$. The computer program for all simulations was written in Prospero Extended Pascal in this laboratory. Graphs were generated using the MINITAB Release 14 Statistical Software.

ization measurements. He pointed out that according to the definition of polarization, in order to measure a polarization of 0.05 with a precision of 1%, $I_{\parallel}$ and $I_{\perp}$ must be known to within 1 part in 1000. Weber classified the systematic errors into three categories, namely:

1. Errors resulting from faulty settings of the parts (by which he specifically meant orientation of the polarizers).
2. Errors resulting from nonnegligible size of the source (by which he meant the aperture effect; *see* **ref.** *8* for a recent discussion of this effect).
3. Errors resulting from stray light (*see* **ref.** *8* for a recent discussion).

Weber applied rigorous propagation of error treatment to all of these potential errors, and the serious student of polarization determinations should read this classic paper. The effect of different types of polarizers and photon counting statistics on polarization measurements was discussed by Jameson et al. *(22)* in their description of the first photon-counting polarization instrument. In this chapter, we shall extend these discussions of measurement errors by explicitly considering the effect of specific errors or uncertainties on the final estimate of the fraction of bound ligand, and hence on the estimated dissociation constant of the ligand–protein complex.

3.2. Modeling of Uncertainties in Determination of Dissociation Constants

One possible way to assess the accuracy and reliability of fluorescence anisotropy and polarization data is the development of an error propagation model. Such a model can provide information about the sensitivity of individual input parameters, as well as a quantitative measure of the quality of the output, i.e., the binding parameters. We note that Tetin and Hazlett *(23)* have presented an excellent discussion of ligand binding in the context of antibody/hapten interactions, and have pointed out the effect of errors in the concentration of bound ligand upon the dissociation constant. Our present treatment shall extend their analysis and, in particular, shall consider the effect of errors in the experimental parameters on the resolved binding parameters.

First, we will formalize the notion of error propagation in general, and then we will employ the generalized model to describe the uncertainties for calculation of binding constants in particular. In this chapter, we use the synonymous terms error, deviation, and uncertainty to represent the variation in measured data. Thus, the term uncertainty indicates absolute error, whereas fractional uncertainty denotes relative error. Percentage uncertainty is the fractional uncertainty multiplied by 100%.

Based on Stoer and Bulirsch *(24)*, we consider a multivariate vector function ϕ, where ϕ is given by m real functions ϕ_i whose values are $y_i = \phi_i(x_1, \ldots, x_n)$, $i = 1, \ldots, m$. We must investigate how the input uncertainties ϕ of Δx affect the

final result $y = \phi(x)$. Suppose component functions ϕ_i have continuous first derivatives. Let $x^{\sim}$ be an approximate value for x. Then we denote the uncertainty of $x_i^{\sim}$ and $x^{\sim}$, respectively by:

$$\Delta x_i = x_i^{\sim} - x \tag{17}$$

and

$$\Delta x = x^{\sim} - x \tag{18}$$

The fractional uncertainty of $x_i^{\sim}$ is defined as the quantity:

$$\varepsilon_{xi} = \frac{\Delta x_i}{x_i} \tag{19}$$

Replacing the input data x by $x^{\sim}$ leads to the result $y^{\sim} = \phi(x^{\sim})$ instead of $y = \phi(x)$. Expanding in a Taylor series and disregarding higher order terms gives

$$\Delta y_i = \sum_j \frac{\Delta x_j \partial \varphi_i(x)}{\partial \chi_i} \tag{20}$$

The quantity $\partial\phi_i(x)/\partial x_j$ represents the sensitivity with which y_i reacts to the uncertainty Δx_j of x_j. If $y_i \neq 0$ for $i = 1,....,m$ and $x_j \neq 0$ for $j = 1,....,n$ then a similar error propagation formula holds for fractional uncertainties:

$$\varepsilon_{yi} = \sum_j \varepsilon_{xj} \frac{x_j}{\varphi_i(x)} \frac{\partial \varphi_i(x)}{\partial \chi_j} \tag{21}$$

The $(x_j/\phi_i)\partial\phi_i/\partial x_j$ indicate how strongly a fractional uncertainty in x_j affects the fractional uncertainty in y_j. The amplification factors have the advantage of not depending on the scales of y_i and x_j.

The amplification factors for relative uncertainties are customarily called condition numbers. If any condition numbers are present which has large absolute values, then the problem is ill-conditioned, otherwise it is well-conditioned. For ill-conditioned problems, small relative errors in the input data x can cause large relative errors in the results $y = \phi(x)$. The condition number is meaningful only for nonzero y_i, x_i. It cannot be easily realized for many purposes, because the condition of ϕ is described by m x n numbers. For these reasons, we will present the conditions of particular problems in a more convenient fashion using contour plots to describe the uncertainties in the determination of dissociation constants.

Because fluorescence anisotropy is an additive property, we also have to consider the propagation of uncertainties for additive operations, $\phi(u,v) = u \pm v$. The fractional uncertainty specializes to

$$\varepsilon_{u\pm v} = \frac{u\,\varepsilon_u}{u \pm v} \pm \frac{v\,\varepsilon_v}{u \pm v} \tag{22}$$

The fractional uncertainties of the components do not propagate strongly into the results, provided the components u and v have the same sign. The condition numbers $u/(u+v)$, $v/(u+v)$ then lie between 0 and 1 and they add up to 1, whence

$$\left|\varepsilon_{u\pm v}\right| <= \max\left\{\left|\varepsilon_u\right|,\left|\varepsilon_v\right|\right\} \tag{23}$$

If one component is small compared to the other, but carries a large fractional uncertainty, the result $u + v$ will still have a small fractional uncertainty so long as the other component has only a small fractional uncertainty, i.e., error damping occurs. However, if two components of different sign are added (a rare case in anisotropy and polarization measurements) then at least one of the factors [$u/(u+v)$ or $v/(u+v)$] is bigger than 1, and at least one of the fractional uncertainties will be amplified. This amplification will be extreme if $u = -v$ holds, and therefore cancellation occurs.

3.3. Measurement of Binding Constants

As discussed earlier, if a fluorescent ligand binds to a protein its fluorescence polarization and anisotropy will typically increase to reflect the slower rotation of the ligand–protein complex relative to free ligand. Using either polarization or anisotropy data one can calculate the fraction of ligand bound (x) at any protein concentration. The dissociation constant, K_d, for n identical sites without interaction can then be calculated from x by the expression:

$$K_d = \frac{(1-x)\left(nP_T - xL_T\right)}{x} \tag{24}$$

where P_T and L_T are the total concentration of protein and ligand, respectively. When $n = 1$, the expression reduces to the special (although most common) case of a single binding site. P_T and L_T are value constants in a binding experiment and the primary variable is x on which K_d depends. We must now investigate how uncertainties Δx of x affect the final result, K_d. We start this investigation by considering systematic deviations and random uncertainties alone.

3.4. Systematic Deviations

In recent literature, in particular the literature associated with clinical chemistry applications of the polarization/anisotropy method, we have noted that some investigators analyze their polarization data using the formulation associated rigorously only with the anisotropy function (*see* **ref. 25**). This practice leads to systematic deviations in determination of x and subsequently of K_d. Specifically, direct substitution of polarization values into **Eq. 15**, derived for anisotropy measurements, instead of converting to anisotropies using **Eqs. 7** or

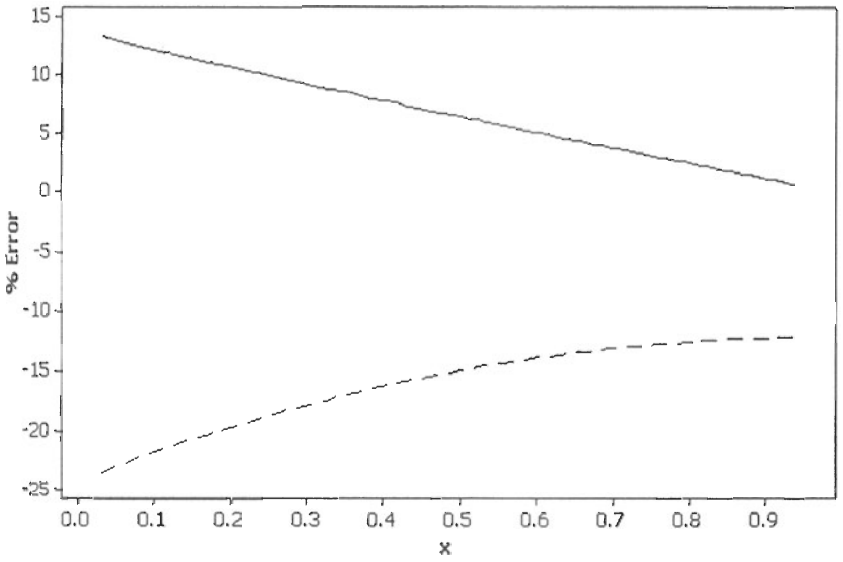

Fig. 3. Percentage error in K_d with respect to direct substitution of polarization in place of anisotropy in the anisotropy additivity equation (**Eq. 15**). Perfect measurement (no input error) is assumed except for the improper substitution. X, fraction of ligand bound; $g = 1$. Solid line, % error in X (direct substitution results in 1–14% overestimation of X); long dashes, % error in K_d (direct substitution results in 12–24% underestimation of K_d). Model parameters are as in **Fig. 2.**

8, or instead of using **Eq. 16** derived for polarization measurements, results in *systematic overestimation of* x *and underestimation of* K_d. This practice is sometimes justified by the rationalization that the attendant errors are not large, yet a systematic examination, using error propagation analysis (analogous to the original treatment of Weber on systematic instrument errors), has not been heretofore presented. In such error propagation treatments, it is customary to present results with a suitable norm, i.e., without their sign. In this chapter, however, we examine the sign of a particular error term as it may give information whether the uncertainty in the result is a case of overestimation or underestimation.

Figure 3 shows ε_K, the percentage deviation in K_d as a function of x and ε_x, the relative deviation in x. ε_x and ε_K were calculated as $(x_p - x_r)/x_r$, and $(K_p - K_r)/K_r$, respectively, and expressed as a percentage. Clearly, it is not enough to simply substitute P for r without taking into account how the particular errors enter into the respective results. Systematic deviations are cumulative in nature. The percentage deviation in x resulting from direct substitution is 1% to 14%

over the whole x range, and the percentage deviation in K_d conditioned on the deviation in x is –12% to –24%. Such deviations may be easily corrected for or eliminated by using the appropriate function to calculate x.

3.5. Precision of Anisotropy and Polarization Determinations

We now will consider uncertainties in the input parameters. As usually practiced, the precision of anisotropy and polarization data is approximately ± 0.002 and ± 0.003, respectively (we note that these are conservative estimates which will vary depending upon the instrumentation utilized, signal strength, and background). Applying the generalized error propagation model described above, ε_x the fractional uncertainty in x with respect to ε_r the fractional uncertainty in r can be calculated by the function:

$$\varepsilon_x = \frac{\varepsilon_r r}{r - r_f} + \frac{\varepsilon_r r(g-1)}{r_b - r_f + (g-1)(r_b - r)} \tag{25}$$

ε_x can be used then to calculate the fractional uncertainty in K_d as follows:

$$\varepsilon_{Kd} = \frac{\varepsilon_x \left(x^2 L_T - nP_T\right)}{(1-x)\left(nP_T - xL_T\right)} \tag{26}$$

We must give a range of possible true values for K_d based on the uncertainties in x. **Figure 4** shows ε_{Kd} as a function of x and ε_x expressed as percentage. As it can be seen, propagation of seemingly small uncertainties in the input parameters can cause larger variations in the results. At low and high values of x, the percentage uncertainty in K_d can be as high as 24% conditioned on a fixed precision of ± 0.002 anisotropy units. Unfortunately, many fluorescence practitioners are not aware of these constraints and mistakenly believe that the precision achievable with modern spectrofluorimeters equates to accuracy in the results. A measurement may be accurate without being precise and vice versa.

For polarization measurements, the fractional uncertainty in x can be derived similarly:

$$\varepsilon_x = \frac{\varepsilon_p P}{P - P_f} + \frac{\varepsilon_p \left[P_b - P_f + (g-1)\left(3 - P_f\right)\right]}{(3-P)\left[P_b - P_f + (g-1)\left(3 - P_f\right)(P_b - P)\right]} \tag{27}$$

This function is more complex than the one for anisotropy measurements and the uncertainty propagates through polarization is slightly larger. The percentage deviation between ε_x calculated from anisotropy and polarization readings is less than 0.5% over the whole x interval though. Therefore, only anisotropy will be considered in the rest of the chapter because of its less convoluted error propagation properties.

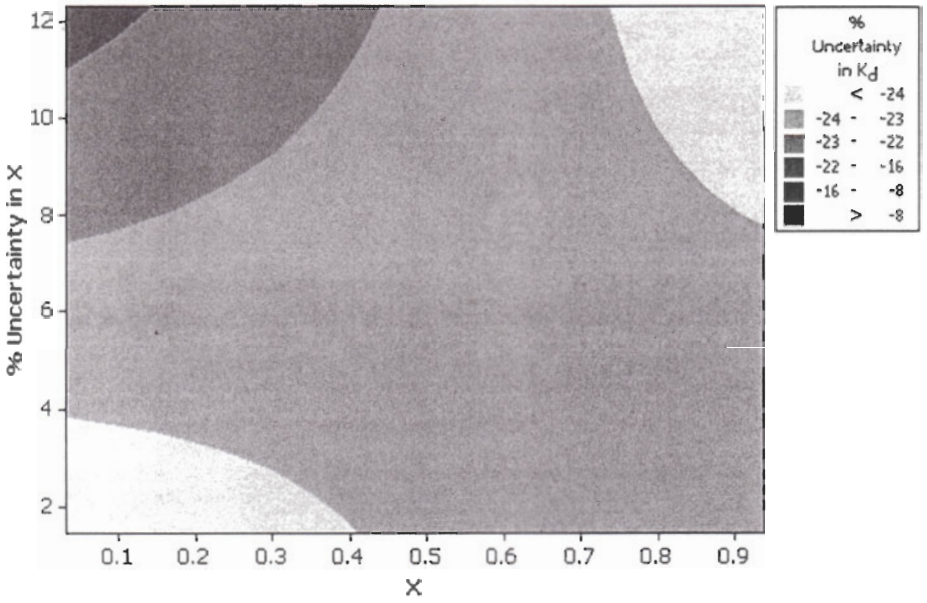

Fig. 4. Percentage uncertainty in K_d with respect to a fixed uncertainty in anisotropy readings. In an otherwise perfect measurement, a fixed uncertainty of +0.002 anisotropy unit is considered, which results in a 8–24% underestimation of K_d. An uncertainty of –0.002 anisotropy unit leads to 8–24% overestimation of K_d. Model parameters are as in **Fig. 2**. X, fraction of ligand bound; $g = 2$.

3.6. Uncertainty in the Anisotropy of the Ligand Free in Solution

Typical anisotropy values for fluorescent ligands free in solution are in the range of 0.02 (*see* **Note 6**), whereas the precision of an anisotropy reading is normally around ± 0.002. Realistically then, approx 10% uncertainties in the value of r_f can be assumed. Again, propagating the errors in r_f, the relative uncertainty in x with respect to ε_f can be calculated by the function:

$$\varepsilon_x = \frac{-\varepsilon_{r,f}\, r_f}{r - r_f} + \frac{\varepsilon_f\, r_f}{r_b - r_f + (g-1)(r_b - r)} \tag{28}$$

and subsequently ε_K can be computed by **Eq. 26**. **Figure 5** shows the effect of uncertainty in the anisotropy of the free ligand on K_d. Since r_f is typically low, K_d is mostly affected at low x values where the observed anisotropy is close to r_f and the amplification factor is higher. The percentage uncertainty in K_d is 5–20% over the entire x range.

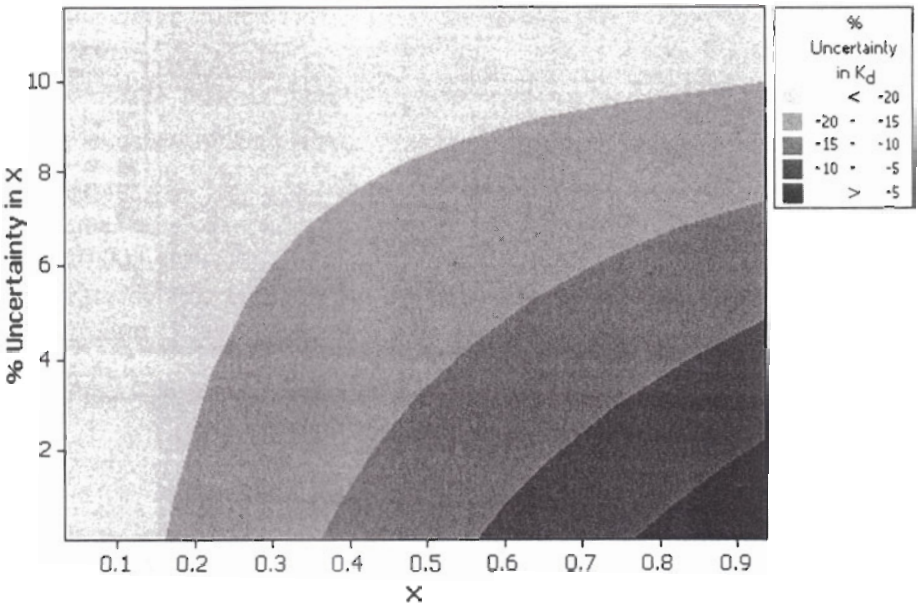

Fig. 5. Percentage uncertainty in K_d with respect to input uncertainties in the anisotropy of the free ligand. A fixed uncertainty of –10% in r_f is considered which results in approx 5–20% underestimation of K_d. An uncertainty of +10% in r_f leads to 5–20% overestimation of K_d. Model parameters are as in **Fig. 2**. X, fraction of ligand bound; $g = 2$.

3.7. Uncertainty in the Anisotropy of the Bound Ligand

Often other uncertainties are larger than the cases considered previously. As the limiting anisotropy is an asymptotic property, relatively small uncertainties in ε_b can propagate into larger deviations in K_d as the observed anisotropy approaches the anisotropy of the bound ligand (*see* **Note 5**). The uncertainty in ε_x with respect to ε_b is given by the function:

$$\varepsilon_x = \frac{-\varepsilon_b\, g r_b}{r_b - r_f + (g-1)(r_b - r)} \tag{29}$$

where the upper bound of the amplification factor equals to g if $r \to r_b$. This fact may lead to considerable uncertainties in ε_x even at moderately low values of g. **Figure 6** shows the dependence of uncertainties in K_d with respect to –5% underestimation of r_b. At x values larger than 0.7, K_d appears to be underestimated by 120–150 %. A + 5% overestimation of r_b would result in 120–150%

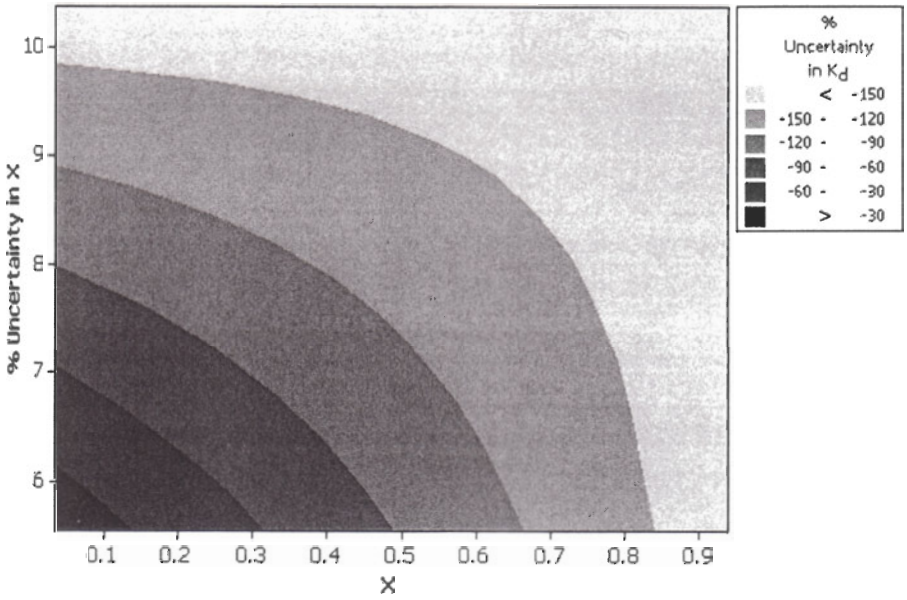

Fig. 6. Percentage uncertainty in K_d with respect to input uncertainties in the anisotropy of the bound ligand. A fixed uncertainty of –5% in r_b is considered which results in 30–150% underestimation of K_d. Similarly, an uncertainty of +5% in r_b leads to overestimation of K_d to the same extent. Model parameters are as in **Fig. 2**. X, fraction of ligand bound; $g = 2$.

overestimation of K_d. Clearly, the fixed value of r_b should be as accurate as possible to minimize uncertainties in K_d.

3.8. Uncertainty in the Fluorescence Enhancement Factor

A further understanding of the accuracy of the calculated binding constants can be obtained by propagating the uncertainties in the enhancement factor, ε_x as a function of ε_g can be calculated by the function:

$$\varepsilon_x = \frac{-\varepsilon_g g\left(r_b - r\right)}{r_b - r_f + (g-1)\left(r_b - r\right)} \tag{30}$$

The amplification factor is small at higher x values and is only moderately high at x values less than 0.3. A 10% underestimation of g results in 12 to 18% underestimation of K_d, whereas a 10% overestimation of g results in a similar 12 to 18% overestimation of K_d. The accuracy of g does not have a major effect

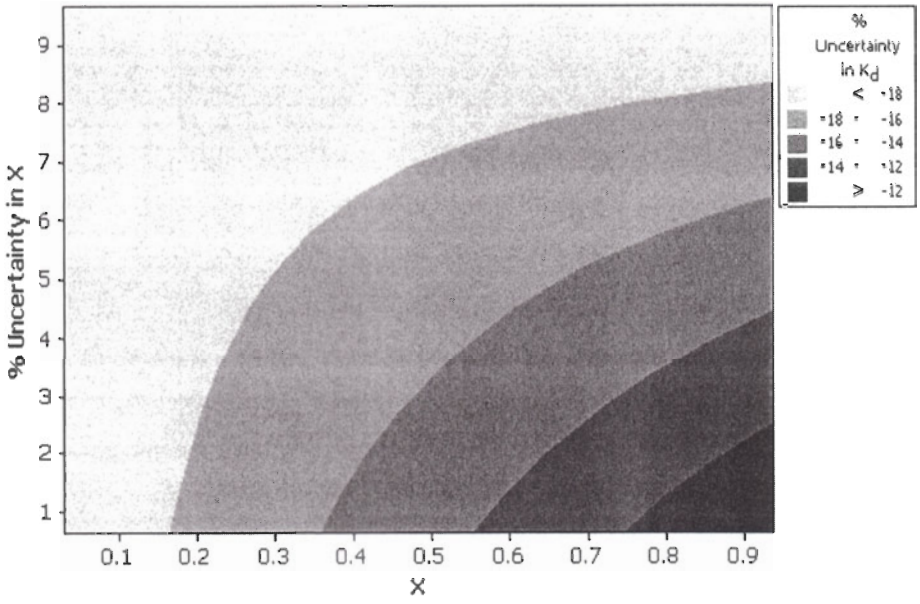

Fig. 7. Percentage uncertainty in K_d with respect to input uncertainties in the fluorescence enhancement factor. A fixed uncertainty of −10% in g is considered which causes 12–18% underestimation of K_d. An uncertainty of +10% in g results in 12–18% overestimation of K_d. Model parameters are as in **Fig. 2**. X, fraction of ligand bound; $g = 2$.

on the final results for K_d when g is the only source of uncertainty. **Figure 7** shows the dependence of uncertainties in K_d with respect to −10% uncertainty in g.

3.9. Modeling of Multiple Uncertainties Together

We now employ the generalized error propagation model to each input parameter jointly. Because the individual input terms has opposing signs and their uncertainties are in a ± value range, the uncertainties in the output cannot be described by a predetermined mathematical model. Rather, it is possible to calculate an upper bound for the joint maximum uncertainty assuming that all input certainties propagate into the same direction, i.e., overestimation or underestimation, respectively. Technically, using absolute norms will have the same effect. The uncertainty of results from any real experiment will be then smaller than the simulated upper bound. Random uncertainties obey the law of probability and tend to cancel or damp each other as discussed earlier. By substituting all individual error terms into **Eq. 26**, ε_{Kd} for the joint uncertainty can

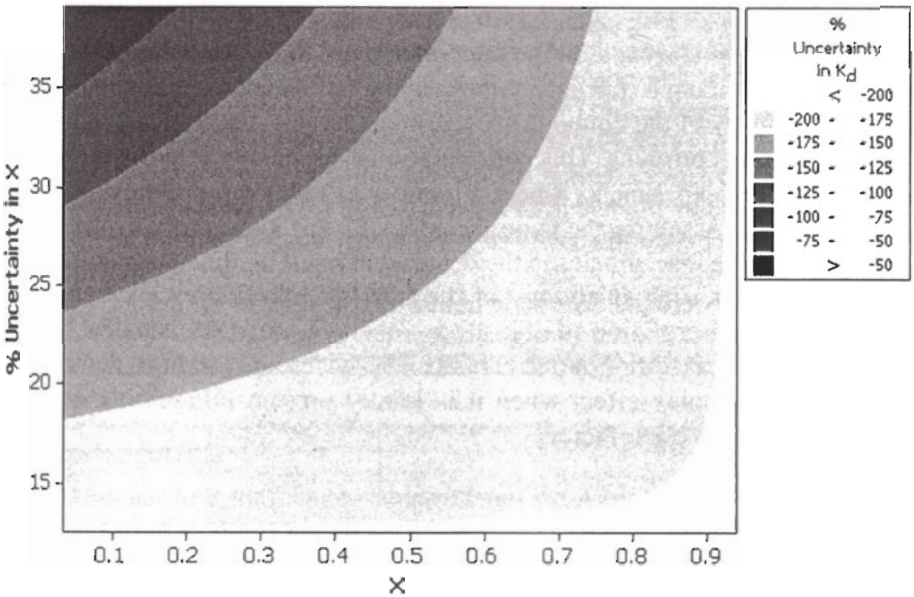

Fig. 8. Upper bound percentage uncertainty in K_d with respect to input uncertainties jointly present in all input parameters. A fixed uncertainty of +0.002 in r, −10% in r_f, −5% in r_b and −10% in g is considered which all propagates to underestimate K_d. At worst case, K_d appears 50–200% lower than its true value. Reversing all signs in the individual error terms leads to overestimation of K_d to the same extent. Model parameters are as in **Fig. 2**. X, fraction of ligand bound; $g = 2$.

be calculated. This effect is shown in **Fig. 8** for K_d using the same input parameters and their respective accuracies as before. Interestingly, the joint upper bound attains a maximum value when x is higher than 0.6 and ε_x is lower then 20% caused by the influence of g on the joint output. In combination with other errors, the uncertainty in g has a larger and biased effect on the common amplification factor, at least with the particular input parameters used for the present modeling.

3.10. Conclusion

An error propagation model has been developed for modeling of uncertainties in determination of dissociation constants. The main parameters are the multivariate functions of typical input constraints for anisotropy measurements. The values of all input parameters as well as their accuracies are needed for the simulation. Each single parameter is investigated separately. It is also possible to perform the error propagation with multiple parameters together. The devel-

opment of the error propagation provides the opportunity to assess the quality of output data conditioned on the uncertainties in the input parameters alone. An important finding is that uncertainties in the estimated or experimental value of the anisotropy of the bound probe cause the largest inaccuracies in the output dissociation constants. This consideration is especially important for large scale screening experiments where a number of unknown proteins are tested simultaneously. Assuming the same anisotropy for the bound probe in all systems may lead to large inaccuracies in the determination of binding constants. Other input parameters such anisotropy of the free ligands, fluorescence enhancement factor, and precision of anisotropy readings propagate smaller but not insignificant uncertainties into the results. The uncertainty in the enhancement factor has a complex effect when it is jointly present in combination with uncertainties from other factors.

4. Notes

1. A critical consideration as regards limiting values of polarization (P_0) or anisotropy (r_0) is that these parameters may have a pronounced wavelength dependence. *See* **refs. *5–8*** for example.
2. For a spherical protein of molecular weight 44 kD, with a partial specific volume of 0.74 and 0.3 mL/mg hydration, at room temperature, one then calculates $\rho = (3)(0.01)(44000)(0.74 + 0.3)/(8.31 \times 10^7)(293) = \sim 56$ ns. So, to a rough approximation the Debye rotational relaxation time (in ns) for a spherical protein is close to its molecular weight in units of kD. In fact, to a rough approximation one can apply this *rule-of-thumb* to systems other than proteins, e.g., if a fluorophore has a molecular weight of 500 daltons, its rotational relaxation time will be (very) approx 0.5 ns. We should also comment here on the term *rotational correlation time*, often denoted as τ_c, is often used in conjunction with anisotropy determina-tions. In fact, $\rho = 3\tau_c$, a fact that stems form the original definitions of these terms *(20)*.
3. The term *fractional contribution* actually refers to the fractional contribution to the photocurrent (or number of photons), which each particular molecular species provides. This contribution does not then strictly refer to the fraction of molecular species present, but will depend upon the absorption and fluorescence spectra of each component, the particular region of the spectrum being monitored, and the response characteristics of the instrument at the relevant wavelength regions. For a discussion of such instrument response characteristics *see* **ref. *3***.
4. Consider a typical small fluorescent ligand with a rotational relaxation time of 1 ns. If the fluorescent lifetime is 0.1 ns, then the polarization observed for the free ligand will be quite high—near the limiting polarization—because the probe does not have time to rotate appreciably before emission. On the other hand, if the probe lifetime is very long (e.g., some pyrene probes can be more than a hundred ns and ruthenium can be hundreds of ns) then both free and bound probes could give very low polarization values.

5. Companies such as Molecular Probes (now part of Invitrogen), for example, specialize in creating literally thousands of fluorescence probes that can be reacted with amines, thiols, hydroxyls, etc. The highest polarization or anisotropy values possible for a fluorescence probe in solution is 0.5 (polarization) and 0.4 (anisotropy), for the case of one photon excitation *(7)*. However, even for the most favorable ratio of probe lifetime to rotational relaxation time, this limit is rarely achieved as a result of the often extensive local mobility of the probe about its point of attachment to the ligand *(9)*. This effect will often lower the observed anisotropy of bound probe to values in the range of 0.3 or lower. Determination of the anisotropy of the bound probe can best be accomplished by measuring the anisotropy when the protein concentration greatly exceeds the ligand concentration and is, furthermore, well above the dissociation constant of the ligand–protein complex *(1)*.

Acknowledgments

DMJ wishes to acknowledge support from the American Heart Association (GIA0151578Z). GM is supported in part by Grant G12-RR03061 (Cadman, Core Support) from the National Institutes of Health.

References

1. Weber, G., 1992, *Protein Interactions*, Chapman and Hall, New York.
2. Winzor, D. J. and Sawyer, W. H. (1995) *Quantitative Characterization of Ligand Binding*, Wiley-Liss, New York.
3. Jameson, D. M., Croney, J. C., and Moens, P. D. (2003) Fluorescence: basic concepts, practical aspects and some anecdotes. *Methods Enzymol.* **360**, 1–43.
4. Oiwa, K., Jameson, D. M., Croney, J. C., Eccleston, J. F., and Anson, M. (2003) The 2'-O- and 3'-O-Cy3-EDA-ATP(ADP) vanadate complexes with myosin S1 are spectroscopically distinct. *Biophys. J.* **84**, 634–642.
5. Valeur, B. (2002) *Molecular Fluorescence*, Wiley-VCH Publishers, Weinheim, Germany.
6. Lakowicz, J. R. (1999) *Principles of Fluorescence Spectroscopy*, Kluwer Academic/Plenum Publishers, New York.
7. Weber, G. (1966) Polarization of the fluorescence of solutions. In *Fluorescence and Phosphorescence* (D. Hercules, ed.), Wiley, New York, pp. 217–240.
8. Jameson, D. M. and Croney, J. C. (2003) Fluorescence polarization: past, present and future. *Comb. High Throughput Chem.* **6**, 167–173.
9. Jameson, D. M. and Seifried, S. E. (1999) Quantification of protein-protein interactions using fluorescence polarization. *Methods* **19**, 222–233.
10. Weigert, F. (1920) Uber polarisiertes fluoreszenzlicht. *Verh. d.D. Phys. Ges.* **1**, 100–102.
11. Perrin, F. (1926) Polarisation de la lumière de fluorescence. Vie moyenne des molécules dans l'etat excité. *Jour de Phys, VIe Série* **7**, 390–401.
12. Laurence, D. J. R. (1952) A study of the adsorption of dyes on bovine serum albumin by the method of the polarization of fluorescence. *Biochem. J.* **51**, 168–177.

13. Dandliker, W. B. and Feijen, G. A. (1961) Quantification of the antigen-antibody reaction by the method of polarization of fluorescence. *Biochem. Biophys. Res. Comm.* **5,** 299–304.
14. Dandliker, W. B. and De Saussure, V. A. (1970) Fluorescence polarization in immunochemistry. *Immunochemistry.* **7,** 799–828.
15. Jolley, M. E., Stroupe, S. D., Schwenzer, K. S., Wang, C. J., Lu-Steffes, M., Hill, H. D., Popelka, S. R., Holen, J. T., and Kelso, D. M. (1981) Fluorescence polarization immunoassay. iii. An automated system for therapeutic drug determination. *Clin. Chem.* **27,** 1575–1579.
16. Weber, G. (1952) Polarization of the fluorescence of macromolecules. 1. Theory and experimental method. *Biochem. J.* **51,** 145–155.
17. Jablonski, A. (1960) On the notion of emission anisotropy. *Bull. Acad. Polon. Sci. Serie des sci. math. astr. et phys.* **6,** 259–264.
18. Mocz, G., Helms, M.K., Jameson, D.M., and Gibbons, I.R. (1998) Probing the nucleotide binding site of axonemal dynein with the fluorescent nucleotide analog 2'(3')-O-(N-methylanthrananiloyl)-adenosine 5'-triphosphate. *Biochemistry* **37,** 9862–9869.
19. Jameson, D. M. and Sawyer, W. H. (1995) Fluorescence anisotropy applied to biomolecular interactions. *Methods Enzymol.* **246,** 283–300.
20. Jameson, D. M. and Eccleston, E. F. (1997) Fluorescent nucleotide analogs: synthesis and applications. *Methods Enzymol.* **278,** 363–390.
21. Weber, G. (1956) Photoelectric method for the measurement of the polarization of the fluorescence of solutions. *J. Opt. Soc. Amer.* **46,** 962–970.
22. Jameson, D.M., Weber, G., Spencer, R.D., and Mitchell, G. (1978) Fluorescence polarization: measurements with a photon-counting photometer. *Rev. Sci. Instru.* **49,** 510–514.
23. Tetin, S.Y. and Hazlett, T.L. (2000) Optical spectroscopy in studies of antibody-hapten interactions. *Methods* **20,** 341–361.
24. Stoer J. and Bulirsch R. (1980) Error propagation. In *Introduction to Numerical Analysis*, Springer-Verlag, New York, pp. 9–20.
25. Prystay, L., Gosselin, M., and Bandks, P. (2001) Determination of equilibrium dissociation constants in fluorescence polarization. *J. Biomol. Screen.* **6,** 141–150.